Electronic Supplementary Material (ESI) for New Journal of Chemistry.

Supporting Information

Solution-processed filamentous copper phthalocyanine films for enhanced NO_2 gas sensor at room temperature

Ziyang Cui [a], Lu Wang [a]*, Yangyang Zhu [a], Yiqun Zhang [a], Li Juan Wang [a]*

a School of Chemical Engineering, Changchun University of Technology, Changchun, 130012, China

* Corresponding author. E-mail address: wlu871227@163.com (L. Wang.)

wlj15@163.com (L. J. Wang.)

Number of pages: 15

Number of figures:10

Number of tables: 1

1. Sensor fabrication and measurement

Au (~ 40 nm) was deposited on the spin-coated CuPc films through shadow mask to form electrodes for transistors. For sensors, 5 pairs (10 conductive channels) finger electrodes with channel length and width of 100 μm and 3 mm were formed on the films. The target gases flow and concentration were controlled by an automatic mixed gas system with original gases and the clean dry (synthetic) air was purchased commercially. The original gases were 1, 5, 10, 15, 20 and 25 ppm NO_2/air. The pure air also acted as the carrier gas. When the carrier gas went through the device (sealed in a box), its velocity was 300 sccm during the test. In the work, the gas-off (pure air) pulse were kept for 10 ~ 30 minutes and the gas-on (target gases) pulses were kept for 10 ~ 30 minutes. The humidity controller controls the humidity of the gas entering the sealed test chamber. The sensors test system illustration was shown in **Figure S1**.

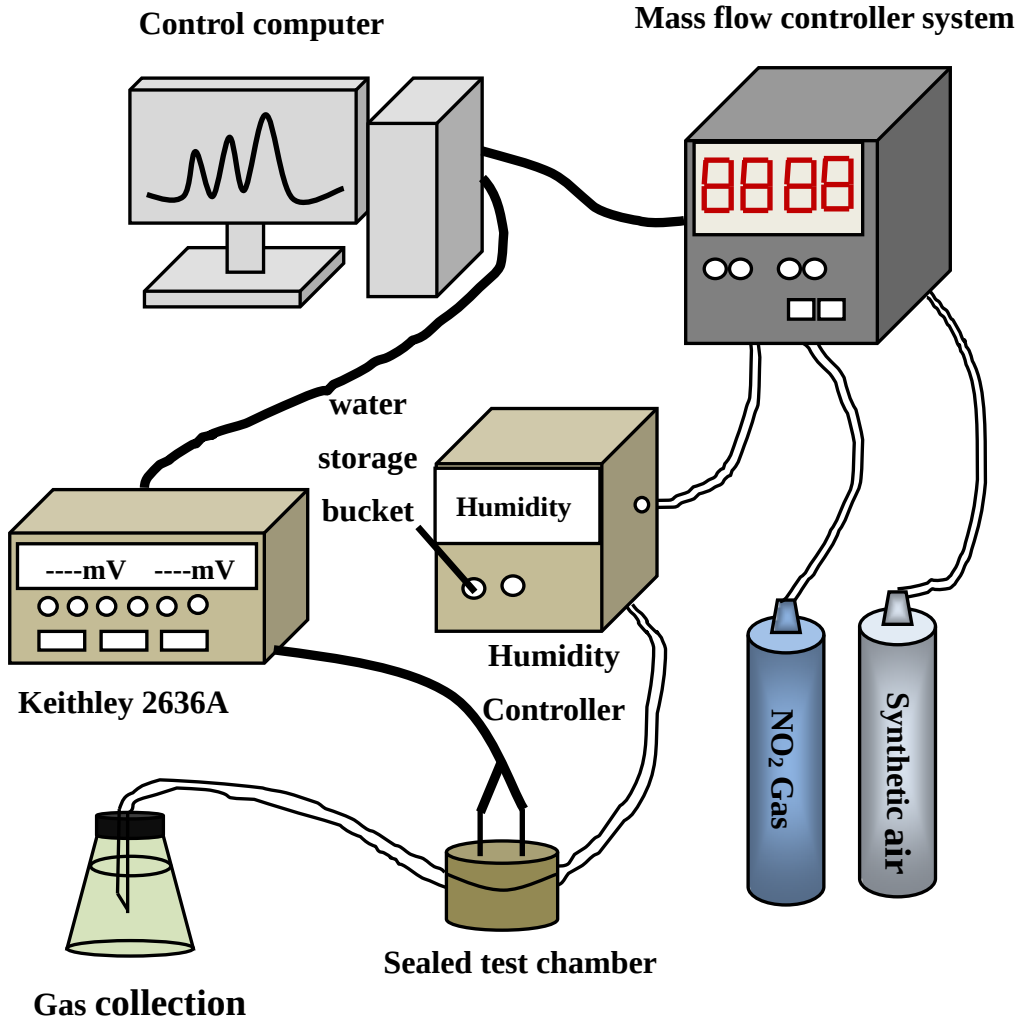

Figure S1. Sensors test system illustration.

2. The morphology characterizations of the filamentous CuPc films

The filamentous CuPc films with different solution concentrations on the SiO_2/Si substrates were fibrous and had different degree of cracks. In order to characterize the crack degree of the filamentous CuPc films, the average ratio of the filamentous CuPc films coverage on the SiO_2/Si substrates was extracted, as shown in **Figure S2**. The mean coverage of the cracks was defined as 100 % minus the coverage of the filamentous CuPc films on the SiO_2/Si substrates. For 45 mg/mL, 75 mg/mL and 105

mg/mL the filamentous CuPc films, the average ratio of cracks was about 12.72 %, 6.98 % and 21.16 %, respectively.

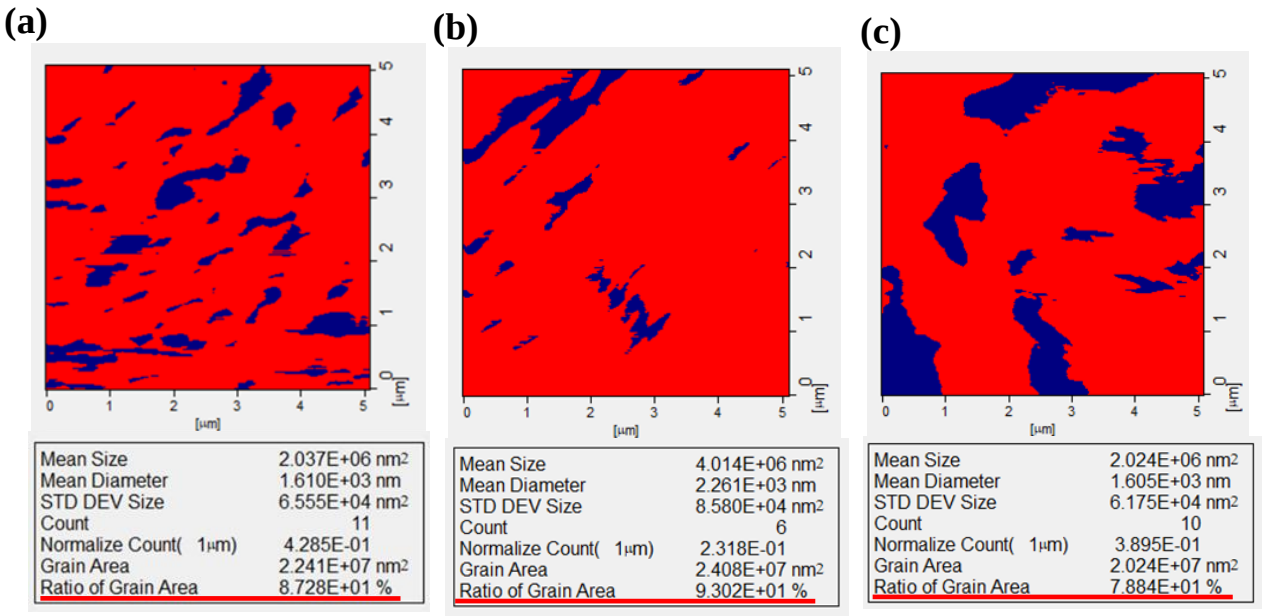

Figure S2. AFM morphology (5 μm ×5 μm) of the filamentous CuPc films based on different concentration of CuPc solution, (a) 45 mg/mL; (b) 75 mg/mL; (c) 105 mg/mL.

In order to further investigate the micromorphology of the filamentous CuPc films, the microstructure of the filamentous CuPc films was investigated by TEM. The resulting images showed that most of the CuPc nanoparticles were uniformly distributed and some were clustered as shown in **Figure S3**.

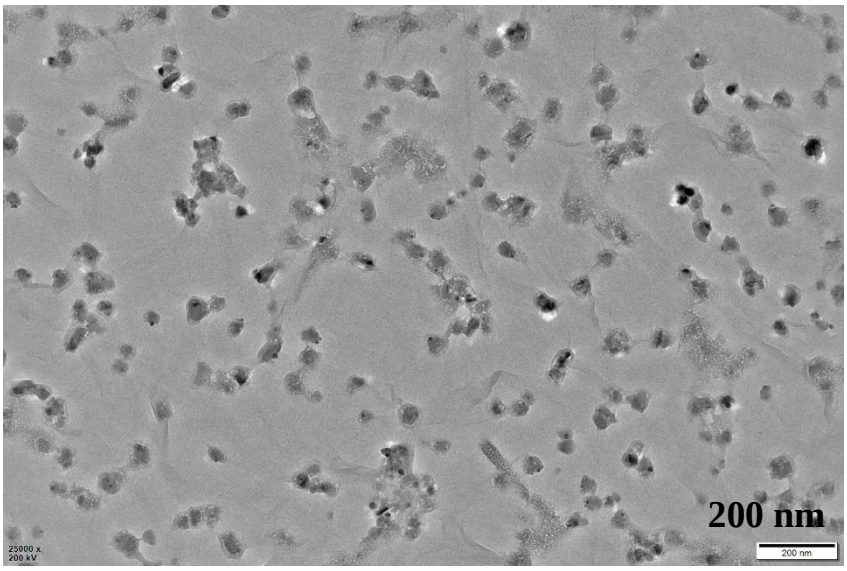

Figure S3. TEM image of spin-coated CuPc films on the SiO_2/Si substrates.

The surface and interface electron states of the filamentous CuPc films were measured and analyzed with an X-ray photoelectron spectroscopy (XPS) instrument (Nexsa, Thermofisher Scientific). To further investigate into the electron states of the filamentous CuPc films, the evolution of the XPS fine spectra of Cu 2p, C 1s and O 1s for the filamentous CuPc/SiO_2 contact as the CuPc solution concentration increased were shown in **Figure S4**, respectively. The Cu 2p peak (Figure S4a) of the filamentous CuPc/SiO_2 contact is fitted into two peaks at 957.12 and 937.24 eV, corresponding to the electron states of Cu $2p_{1/2}$ and Cu $2p_{3/2}$, respectively. From the blinding energy of copper atoms in Cu $2p_{3/2}$ electron state, it could be known that the copper atoms in the filamentous CuPc films were Cu (II) [1]. At the same time, with the increase of CuPc solution concentration, the intensity and peak position of Cu 2p peak remained basically unchanged. The C 1s peak (Figure S4b) of the filamentous CuPc /SiO_2 contact is fitted into two peaks at 287.87 and 285.02 eV. The peak at 287.87 eV was attributed to the N-C=N bond. The peak at 285.02 eV was attributed to the C-C

bond [2]. In addition, a satellite peak was observed at 289.13 eV, which was slightly higher than the binding energy of carbon atom with one carbon atom and two nitrogen atoms. It was believed that this was due to oxidation, and the oxygen atoms might come from the O_2 absorbed by the SiO_2 substrate and the filamentous CuPc films [1]. The peak of the O 1s spectrum was located at a very wide scale of 530.35-536.58 eV, and the O1s spectrum was not very regular (Figure S4c). It was speculated that the reason for the wide spectrum peak of O1s and its development towards higher binding energy was as follows: when the samples were exposed to the atmosphere during the transfer from the vacuum deposition chamber to the XPS analyzer, some O_2 and H_2O were absorbed by the filamentous CuPc/SiO_2 substrate, because the oxygen in O_2 and H_2O had higher binding energy.

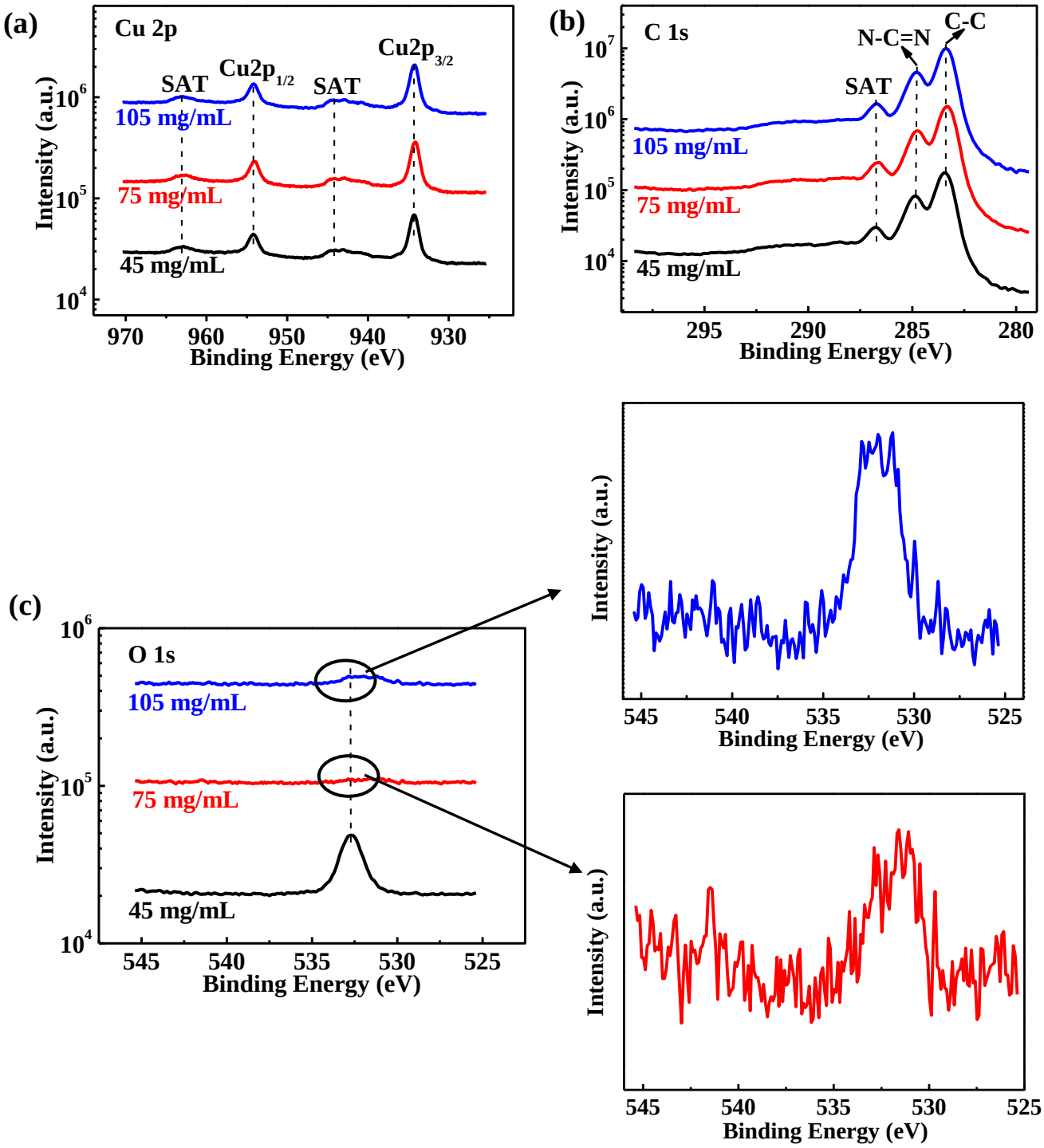

Figure S4. The fine spectra of Cu 2p (c), O 1s (d) and C 1s (e) for the filamentous CuPc films as the concentration of the CuPc solution increases. (SAT-satellite peak).

3. The effect of CuPc solution concentration on electrical properties of the filamentous CuPc films

In order to study the effect of CuPc solution concentration on the electrical properties of the filamentous CuPc films transistors, the electrical properties of the filamentous CuPc films transistors with different CuPc solution concentration were studied. **Figure S5** showed the output and transfer characteristic curves of the filamentous CuPc films transistors with solution concentrations of 45 mg/mL, 75 mg/mL and 105 mg/mL respectively.

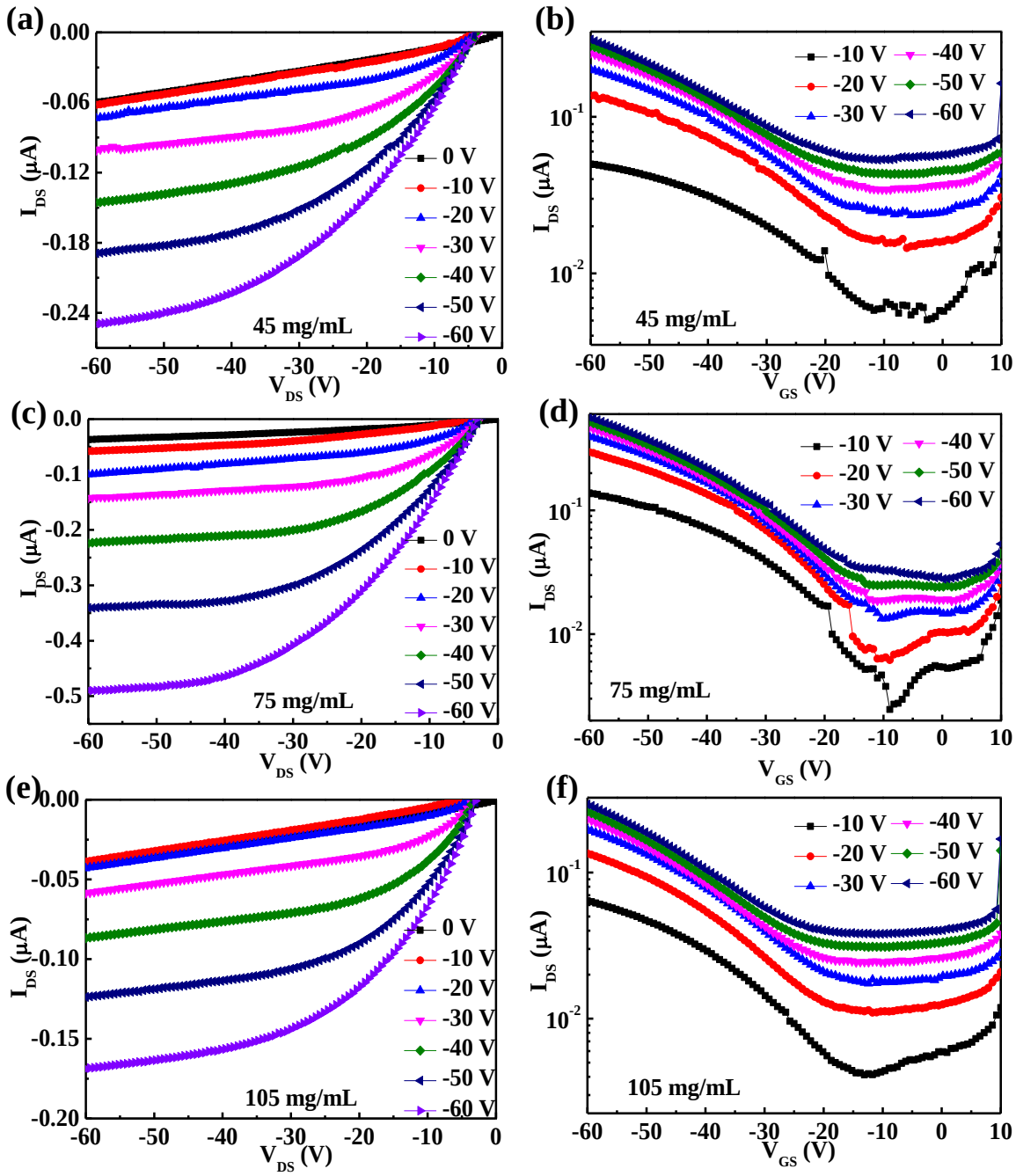

Figure S5. The output curves of the filamentous CuPc OFETs, (a) 45 mg/mL, (c) 75 mg/mL, (e) 105 mg/mL.

The transfer curves of the filamentous CuPc OFETs, (b) 45 mg/mL, (d) 75 mg/mL, (f) 105 mg/mL.

4. Effect of NO_2 gas concentration on electrical properties of the filamentous CuPc films

The influence of different NO_2 gas concentration on the electrical performance of OFETs of the filamentous CuPc films was studied. At NO_2 gas concentrations of 0 ppm, 5 ppm, 15 ppm and 20 ppm, the output and transfer characteristic curves of the filamentous CuPc films transistors with CuPc solution concentration of 75 mg/mL were shown in **Figure S6** and **Figure S7**, respectively. The study of electrical properties is helpful to further analyze the response mechanism of the filamentous CuPc films sensors.

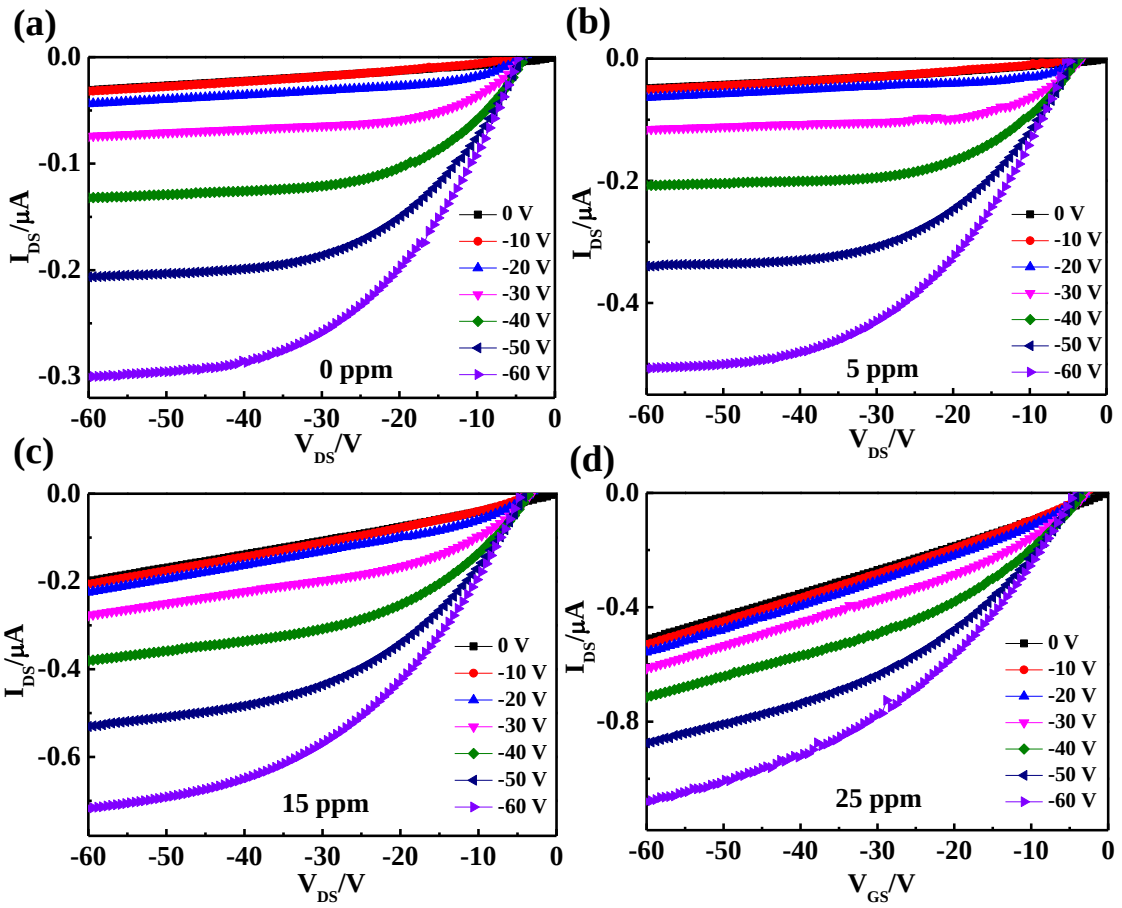

Figure S6. The output curves of the filamentous CuPc OFETs upon exposure to NO_2 gas at various concentrations. (a) 0 ppm, (b) 5 ppm, (c) 15 ppm, (d) 25 ppm.

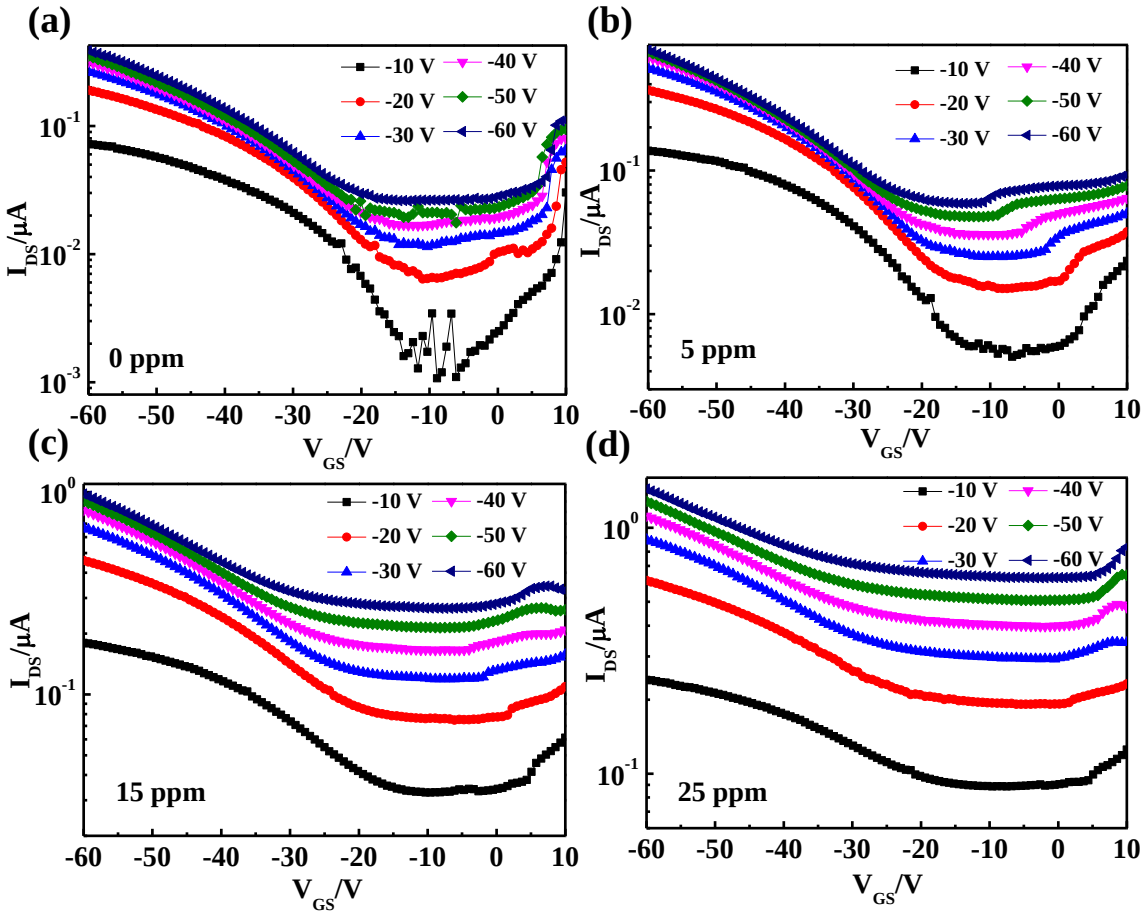

Figure S7. The transfer curves of the filamentous CuPc OFETs upon exposure to NO_2 gas at various concentrations. (a) 0 ppm, (b) 5 ppm, (c) 15 ppm, (d) 25 ppm.

5. The response recovery curves of the filamentous CuPc films sensors

The response recovery curves of the filamentous CuPc films sensors with CuPc solution concentrations of 45 mg/mL and 105 mg/mL to dynamic concentration NO_2 gas were shown in **Figure S8**. The sensors had good response to NO_2 gas, but the baseline drift was obvious, and the resilience of the sensors needs to be improved.

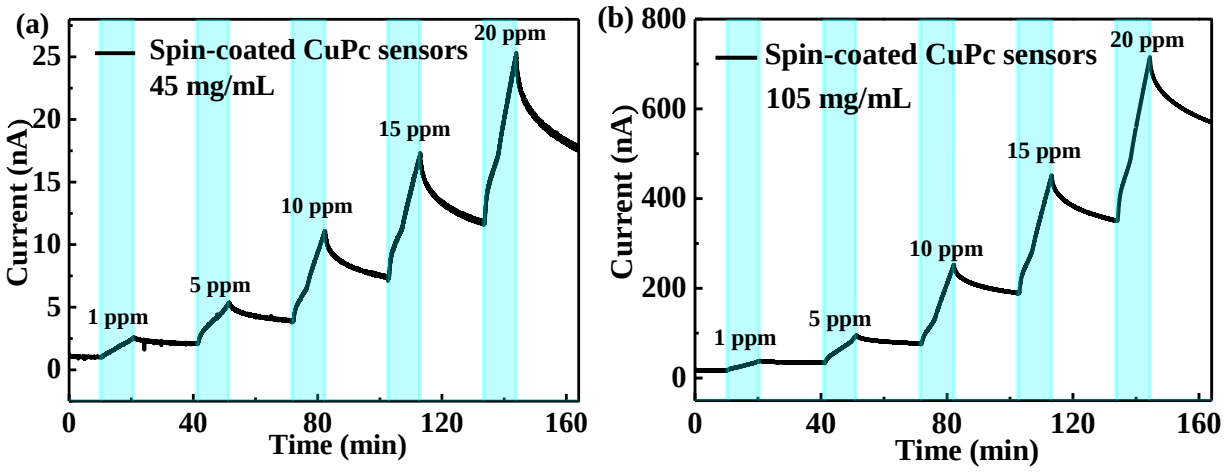

Figure S8. Dynamic response-recovery curves of OFET sensors based on the filamentous CuPc films to different concentration of NO_2 at room temperature, (a) 45 mg/mL, (b) 105 mg/mL.

6. The linearity of the filamentous CuPc-based OFETs sensors

The dynamic response curves of resistance based on the filamentous CuPc films sensors with 75 mg/mL CuPc solution concentration were shown in **Figure S9**. The the filamentous CuPc films sensors presented a certain degree of linear sensing in response to gas concentration with the coefficient of determination $R^2 \approx 0.907$.

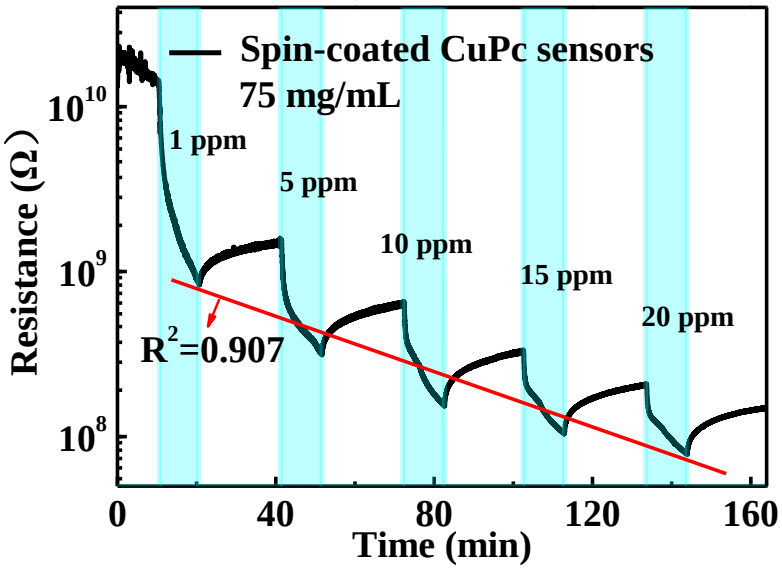

Figure S9. Dynamic response curves of resistance based on the filamentous CuPc films sensors with 75 mg/mL CuPc solution concentration

7. Change of sensing effect of the filamentous CuPc films sensors with time

Dynamic response curves of the filamentous CuPc films sensors for 0, 4, 8 and 16 days sensing 10 ppm NO_2 were shown in **Figure S10**. It could find that the responsivities of the filamentous CuPc films sensors to NO_2 at 10 ppm had little change with time.

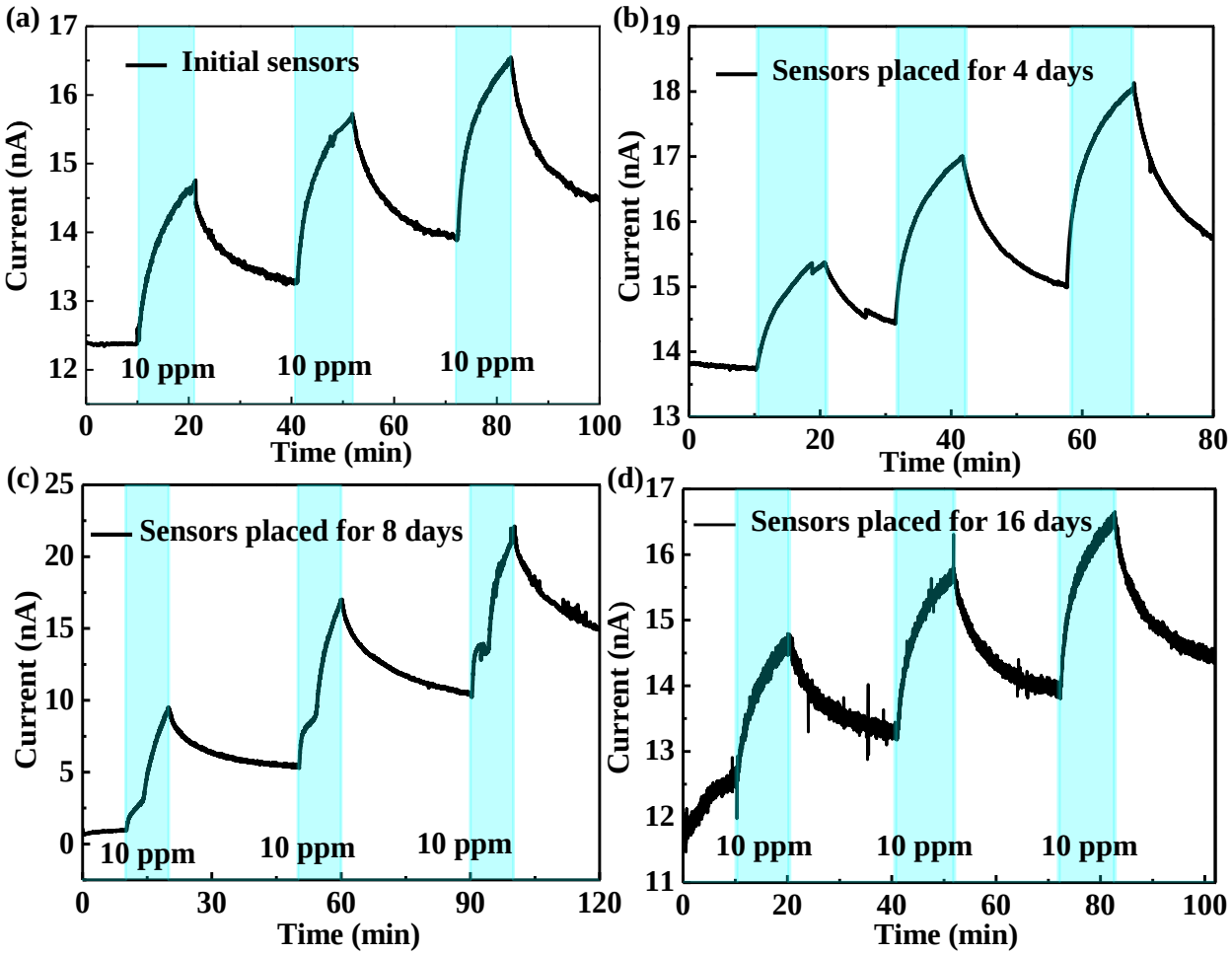

Figure S10. The atmosphere stability of the filamentous CuPc films sensors was tested in the placed days during 16 days. Continuous test stability curves of the filamentous CuPc films sensors at 10 ppm and at room temperature (25 ℃) and 35 % RH.

8. Summary of sensors in recent years

To understand the advantages of the spin-coated CuPc films sensors, the relevant information of series of sensors reported in recent years was summarized, as shown in **Table S1**.

Table S1. Comparison of some recent reported semiconductors gas sensors of different types.

Materials	Operating temperature (℃)	Detection limit	Target gas	Ref.
spin-coated CuPc film	RT	0.3 ppm	NO_2	Our work
rGO/F16CuPc	RT	1.41 ppb	Cl_2	3
N-doped SnO2-rGO nanohybrids	120	0.5 ppm	NO_2	4
CuPc/ ordered PVA nanofibers	RT	0.3 ppm	NO_2	5
CuPc/p-6P/ Al_2O_3/PMMA	RT	1 ppm	NO_2	6
Cu/ZnO/rGO nanocomposites	200	1 ppm	NO_2	7
reduced graphene oxide/cobalt phthalocyanine hybrids	RT	30 ppm	NH_3	8
3D open porous SnO_2	160	5 ppm	Cl_2	9
In_2O_3 nanosheets	200	3 ppm	Cl_2	10
ZnO nanowires	RT	0.5 ppm	NO_2	11
tetrapyrene porphyrins nano-petal and spherulofloral	RT	50 ppb	NO_2	12

References

1 J. Marsh, L. Minel, M.G. Barthes-Labrousse and D. Gorse , Appl. Surf. Sci. 1998, 133, 270-286.

2 J.F. Watts and J.E. Castle, J. Mater. Sci. 1984, 19, 2259-2272.

3 S.Kumar, A. K. Sharma, M. K. Sohala, D. P. Sharma, A. K. Debnath, D. K. Aswal and A. Mahajan, Sensor. Actuat. B-Chem., 2020, 128925.

4 M.Modak and S. Jagtap, Ceram. Int., 2022, 25, 19978–19989.

5 L. Wang, L. H. Wang, G. Li, Y. Zhu, C. Liu, L. Zeng, S. Zhong and L. J. Wang. Sensor. Actuat. B-Chem., 2021, 337, 129781.

6 Q. Xie, L. Wang, Y. Zhu, Q. Sun and L. Wang, Org. Electron., 74, 2019, 69-76.

7 M. Modak, S.Mahajan, M. Shinde, S. Rane and S.Jagtap, J. Mater. Sci: Mater. Electron., 2022, 33, 26205-26224.

8 E. Yabas¸, E. Biçer and A. Altındal, J. Mol. Struct., 2023, 1271,134076.

9 W. Zhang, Q. Li, C. Wang, J. Ma, C. Wang, H. Peng, Ceram. Int. 2019, 45, 20566-20574.

10 J. Ma, H. Fan, W. Zhang, J. Sui, C. Wang and M. Zhang, Sensor. Actuat. B-Chem., 2020, 305, 127456.

11 M.W. Ahn, K.S. Park, J.H. Heo, D.W. Kim, K.J. Choi and J.G. Park, Sensor. Actuat. B-Chem., 2009, 138, 168-173.

12 Q. Sun, Q. Liu, L. Gong, C. Wang, X. Kong, C. Yang, W. Feng, D. Qi, F. Dai, X. Li, Y. Chen, ChemNanoMat, 2019, 5, 1408-1417.